Natural Hazards (2022) 114:941–969
https://doi.org/10.1007/s11069-022-05418-4

ORIGINAL PAPER

Development of a three-dimensional basin model to evaluate the site effects in the tectonically active near-fault region of Gölyaka basin, Düzce, Turkey

Karim Yousefi-Bavil[1] · Mustafa Kerem Koçkar[2] · Haluk Akgün[1]

Received: 9 September 2021 / Accepted: 22 May 2022 / Published online: 13 June 2022

Abstract
The high seismicity and tectonic activity of the study area located in a near-fault region in Gölyaka, Düzce, results in a bedrock geometry highly complex in the sense of faulting and deformation. This makes this area very challenging in terms of a site response study that would aid seismic hazard assessment. This study develops a basin model to evaluate the site effects in the tectonically formed Plio-Quaternary fluvial sedimentary layers of the Gölyaka region. The selected site uniquely falls within the near-field domain of a section of the North Anatolian Fault System. To determine the presence of these lateral variations in the geology as well as the geometry of the basin over a wide area, surface seismic measurements and deep vertical electrical sounding along with geotechnical boring studies have been performed, and a 3D basin geometry model was developed. The basin model shows that the sediment thickness continues to a depth of approximately 250–350 m with an irregular geometry due to over-step faulting near the southern boundary of the basin. Consequently, this study confirms the spatial variations in the near-field area that depend on basin geometry, material heterogeneity, and topography, indicating dipping and nonuniform stratification in the velocity profiles. Furthermore, the conducted microtremor measurements were used to compare the natural periods of microtremor results, along with interpolated Vs profiles to validate estimated basin depths. In conclusion, this study indicates that a well-developed basin geometry that reflects the complex process associated with the characteristics of the near-fault region could be accurately and reliably determined by developing a 3D basin model to assess site response in an account for seismic hazard assessment studies.

Keywords Near-fault site effects · 3D basin model · Deep vertical electrical sounding · Active and passive surface wave method · H/V microtremor measurements · Gölyaka basin of Düzce-Turkey

✉ Haluk Akgün
hakgun@metu.edu.tr

[1] Geotechnology Unit, Department of Geological Engineering, Middle East Technical University (METU), Ankara, Turkey

[2] Geotechnics Division, Department of Civil Engineering, Hacettepe University, Ankara, Turkey

1 Introduction

Studies in the last few decades have demonstrated that local site conditions, particularly those close to earthquake-prone areas, can generate substantial amplification and spatial variations of earthquake ground motion that considerably affect the level of ground shaking (e.g., Pratt et al. 2003; Ajala and Persaud 2021). Hence, the amplification of ground motion due to local site effects (i.e., basin geometry, topography, and ground motion resonance) plays a crucial role in enhancing seismic damage (Rodríguez-Marek et al. 2001; Bakir et al. 2007; Koçkar and Akgün 2012; Núñez et al. 2013; Eker et al. 2015; Koçkar 2016). Almost all of the destructive earthquakes in the last three decades (e.g., earthquake events such as Kobe 1995; Chi-Chi 1999; Kocaeli and Düzce 1999; Sichuan 2008; New Zealand 2010; Van 2011; Tohoku 2011) have brought particular attention to the significance of site effects. Hence, it is essential to obtain detailed information from the local site conditions to understand the variations of ground motion. In many circumstances, it is widely accepted that site characterization based on shear wave velocity is one of the critical factors in determining the intensity of ground shaking (Joyner et al. 1994; Dobry et al. 2000; Borcherdt 2002). Thus, this is a practical parameter for characterizing local soil conditions for ground motion studies (Park and Elrick 1998; Wills et al. 2000, 2015; Rahman et al. 2018; Biswas et al. 2018). In particular, seismic surface wave velocity is frequency dependent, and wave propagation relies on the dispersive nature of Rayleigh-type surface waves in layered media (Seligson 1970). This dispersive character of surface waves can be effectively utilized to produce a one-dimensional velocity model for a particular site (Rodríguez-Marek et al. 2001; Herak 2008; Boaga et al. 2010; Roy et al. 2013; Pegah and Liu 2016). These estimations have been prepared by using data obtained through array applications, where it should be noted that in some situations where the topography and basin structure are more complex (i.e., tectonically deformed areas in near-fault regions), 2D and 3D basin models are required to account for the lateral heterogeneities or the complex structures that may strongly affect the local ground shaking pattern (Gazetas et al. 2002; Singh et al. 2011; Piatti et al. 2013; Eker et al. 2015; Wang et al. 2016; Narayan and Kamal 2018; Cushing et al. 2020; Mori et al. 2020).

High seismic activity in a near-fault region makes it much more challenging to evaluate the local seismic hazard compared to areas situated at farther distances. Particularly in a near-source region, rupture front and slip direction may have forward directional effects on the ground motion if they are oriented towards the area of interest (Bradley and Cubrinovski 2011). Furthermore, due to tectonic deformation, any seismic velocity model that takes the form of a velocity contrast with a lower velocity zone would be significantly complex in terms of site-specific ground motions at regions located in the proximity of a fault or within a low-velocity fault zone (Dreger et al. 2007). Therefore, the crucial step in hazard estimation for sites near earthquake-prone areas is to reliably determine the basin geometry and define the alluvial and bedrock interface.

The study area is located in the Gölyaka basin in the Eastern Marmara region. It falls within the near-field portion of the NAFS (i.e., up to 8 km next to the rupture at furthest), which is one of the most significant transform fault systems in the world, that produces devastating earthquakes such as the 1999 Kocaeli ($M_w = 7.4$) and Düzce (M_w 7.2) earthquakes. The surface ruptures of the 1999 Kocaeli and Düzce earthquakes form the boundaries of the tectonically formed Gökyaka basin (Akyüz et al. 2002; Barka et al. 2002) in the near field in the south and the northwest, respectively, which makes this location unique and intriguing from a site effect point of view. In general, the westward propagating seismic

activity along the NAFS starting from the 1939 Erzincan earthquake ($M_s = 7.9$), and lately the 1999 Kocaeli and Düzce earthquakes have triggered more than ten severe earthquakes during this century, which have led to more than 50,000 casualties (Barka 1996; MTA 2003). This is one of the most important motivation for studying the Gölyaka basin, which is representive of a unique area for determining non-linear behavior (i.e., velocity anomaly/contrast due to tectonic deformation) resulting from high seismicity in a near-fault region.

This research has assessed the local site conditions and the dynamic characteristics of the sediment (fundamental frequency of site) in the Gölyaka basin and then developed a 3D basin model based on the successfully obtained 1D Vs profiles. In particular, it has focused on areas located at different positions concerning the basin margins; more specifically, areas at the northern and southern boundaries (fault-controlled basin margins) and in an area at the deepest part of the basin. The high resolution Vs profile was obtained by using a combination of active multichannel analysis of surface wave (MASW) and passive microtremor array method (MAM) measurements at a total of 29 locations. These techniques were adapted to satisfy the demands of maintaining a reasonably high sensitivity of shear wave velocity (Park et al. 2007; Gosar et al. 2008; Eker et al. 2012). At 14 locations, the Schlumberger vertical electrical sounding (VES) technique was applied to evaluate the depth of the basin bedrock. In addition, geotechnical data at 30 boring locations incorporating deep engineering geological boring results along with geological and basin topography data have been used to correlate with the Vs profile and the VES model. Then, the microtremor data measured in the study site have been used to verify the inferred basin depth. Finally, these comprehensive survey results led to a well-developed 2D and 3D geometry of a basin model in the Gölyaka basin.

It should be stated that this work is part of the first author's dissertation in partially fulfilling the requirements for a Ph.D. degree in Geological Engineering (Yousefi-Bavil 2022). A part of this dissertation, including geophysical characterization studies, was previously published as a conference article (Yousefi-Bavil et al. 2018).

2 Seismotectonics and seismicity

The study area is located in the Gölyaka basin and is uniquely situated within the bifurcated portion of the North Anatolian Fault System (NAFS). The reason for this uniqueness is that the eastern end of the surface rupture of the 1999 Kocaeli earthquake ($M_w = 7.4$) had terminated in the eastern part of the Gölyaka basin (Fig. 1, 1999 a), and the western end of the surface rupture of the 1999 Düzce earthquake ($M_w = 7.2$) had also initiated in the western part of the study area (Fig. 1, 1999 b).

The NAFS, an active right-lateral strike-slip fault system, is connected to the northward-to-west-extending Anatolian block. The North Anatolian Fault System is divided into two main branches from the west of Bolu district, namely the Düzce fault in the north and the Mudurnu fault in the south. The northern Düzce fault continues by passing through the study area. This fault is in the proximity of the Karadere segment, which is the eastern part of the Kocaeli surface rupture. The Karadere segment and the Düzce fault constitute two diverging strike-slip strips connected by a no-step-over fault junction. This geometric sequence entails a releasing fault wedge, whose long-term morphological expression is represented by the wedge-shaped basin of the Gölyaka region (Fig. 1) (Pucci et al. 2007). The Düzce fault shows up in the east to join the single trace of the NAFS with a right-releasing step-over created by the Bakacak and Elmalık faults

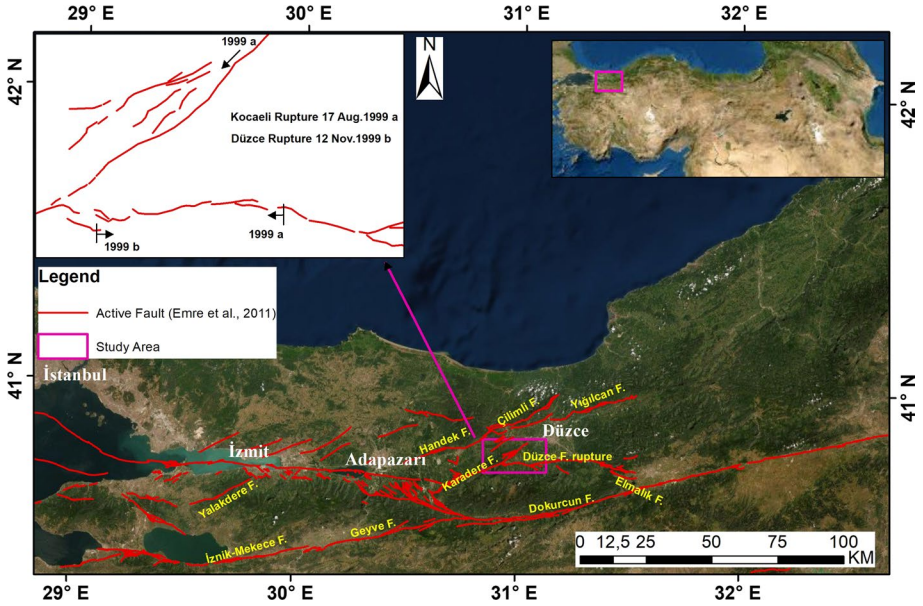

Fig. 1 The western part of the North Anatolian Fault System (NAFS) that is situated within the Eastern Marmara Region (Gürer et al. 2006; Emre et al. 2011) and the epicenter information of the major earthquakes (reproduced from KOERI 2020). It should be noted that the rectangular area displays a close-up view of the bifurcated section of the NAFS in the Gölyaka basin

in the WNW–ESE direction. Contrarily, the western section of the fault extends from the WSW–ENE striking Karadere segment, which borders the İzmit fault. This western boundary of the Düzce fault section sets up a complex right releasing step-over with the Karadere segment that supposedly has clogged the propagation of the Kocaeli earthquake fault rupture (Lettis et al. 2002). Consequently, this releasing zone controls the present-day Düzce basin depocenter Efteni Lake, situated in the study area (Pucci et al. 2007).

The rupture width of the Düzce earthquake has been determined to be 10 km from the seismic data and between 14 and 24.5 km from the literature (Bürgmann et al. 2002; Utkucu et al. 2003). The study area includes major seismic events that can be sorted from the most recent to the past as follows: the 12 November 1999 Düzce ($M_w = 7.2$), the 17 August Kocaeli ($M_w = 7.4$), the 22 July 1967 Mudurnu ($M_w = 6.2$), the 18 September 1963 Yalova ($M_w = 6.2$), the 26 May 1957 Bolu-Abant ($M_w = 6.7$), the 1 February 1944 Bolu-Gerede ($M_w = 6.8$), and the 20 June 1943 Hendek ($M_w = 6.4$) earthquakes (KOERI-RETMC 2020; Fig. 1).

The 1999 Kocaeli earthquake has caused surface ruptures ranging from 40 to 145 km in length, resulting in a total surface rupture length of 185 km (Akyüz et al. 2002; Barka et al. 2002). The horizontal displacement of the rupture surface was around 5 m in the vicinity of the epicenter of this earthquake in Gölcük and around 1.2 m in the east of the Gölyaka region (Polat et al. 2002; Cambazoğlu et al. 2016). A second catastrophic earthquake was the Düzce Earthquake, which occurred on November 12, 1999, approximately three months after the 1999 Marmara earthquake. This earthquake produced a 3.0 m horizontal displacement, a 5.0 m vertical displacement, and a rupture surface length of 45 km (Taymaz 2000). The distance between the eastern end of the 17 August Kocaeli earthquake

rupture line (fault trace) and the western end of the Gölyaka region rupture line is about 9 km (Barka 1996).

These events have caused significant casualties and substantial economic losses (Ambraseys and Zatopek 1969; Barka and Kadinsky-Cade 1988; Akyüz et al. 2002; Barka et al. 2002; Kondo et al. 2005; Palyvos et al. 2007). The 1999 Kocaeli ($M_w = 7.4$) and Düzce earthquakes ($M_w = 7.2$) resulted in significant damage and loss of life within the Eastern Marmara Region. A total of 18, 373 people lost their lives in the Kocaeli earthquake. An additional 710 people lost their lives in the Düzce earthquake that occurred only 87 days later. The number of buildings with 4 to 8 storeys which did not comply with the building code regulations and completely collapsed or were severely damaged, was very high. Specifically, due to the Kocaeli earthquake, 105 people died, and 250 were injured in the Gölyaka district. About 40% of the houses were damaged. More specifically, 878, 345, and 409 houses were heavily, moderately and slightly damaged, respectively (Özmen 2000). Although the Gölyaka district is far from the earthquake's epicenter, the damage was quite severe since it is located in a near-fault region. Due to the earthquake, one person died, and 68 people were injured in the Gölyaka district. A total of 123 heavily damaged, 89 moderately, and 299 slightly damaged buildings were recorded (Aydan et al. 2000).

3 Geological setting

The Gölyaka basin is comprised of unconsolidated Plio-Quaternary deposits intercalated with gravel, sand, silt, and clay that overlie older geological formations as a result of the fluvial activity (Figs. 2, 4). The Quaternary deposits are composed of fluvial, lacustrine, and river delta sediments. The fluvial sediments primarily consist of gravel and sand material in the alluvial fans. However, the deposits of the Düzce basin are composed of thick layers of lacustrine and deltaic sediments, which primarily consist of silt and clay material (Figs. 2, 4). The thickness of the fluvial deposits (relatively coarser material) becomes thicker towards the NE, whereas the lacustrine (fine-grain material) sediments become dominant towards the SW.

In the study area, the Cretaceous units are over-thrusted on the Eocene Yığılca Unit (Ty; andesites, basalts) and the Çaycuma formation (Tc; sandstones, mudstones, and limestones). The Quaternary alluvium and the unconsolidated Plio-Quaternary Karapürçek formation lie unconformably over the older units. The main geologic structure in the study region is the E–W striking northern section of the Düzce fault in the North Anatolian Fault System. The Düzce fault has a fundamental importance in the structural deformation and geomorphological evolution of the region. This dextral strike-slip fault and in some segments with its normal components forms the Düzce plain, which is an extensional Plio-Quaternary basin filled with sediments with a thickness of up to 260 m (Şimşek and Dalgıç 1997).

Figure 3a presents a general view of the study region in the Gölyaka basin and Efteni Lake. As illustrated in this figure, a large part of the study area is situated within the catchment area of the lake (i.e., marshy, reddish-colored area) towards the SE. In general, the area possesses heavy vegetation (it should be noted that in Fig. 3, areas that lack vegetation are located at the margins of the basin (Fig. 3b, c), and the unconsolidated fluvial deposits exist near the main rivers (Fig. 3d, e).

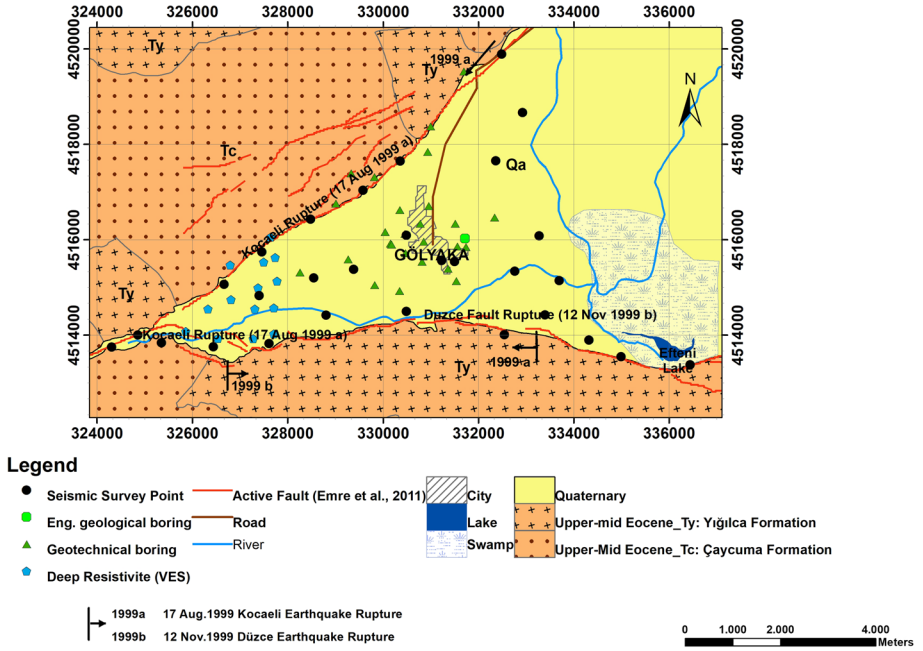

Fig. 2 The geological map of the Gölyaka basin (modified from MTA, A.U., 1999). Note that the black dots display the MASW and MAM test locations, light green dot displays the deep engineering geological boring location, the dark green triangles show the locations of the geotechnical boring data, and the blue dots display the vertical electrical sounding (VES) measurement points (Modified from Yousefi-Bavil et al. 2018; Yousefi-Bavil 2022)

4 Data and methods

The field testing and data analysis were performed on different dates. All field test measurements have been carried out from 2015 to 2019. These field data were utilized to assess the local site conditions and the dynamic sediment characteristics to develop a basin geometry model of the study area by conducting geophysical and geotechnical studies complemented by a thorough geological reconnaissance of the study site (Fig. 2).

4.1 Engineering geological and geotechnical boring study

To investigate the subsurface sediments in the study area, a total of 30 geotechnical (< 15 m in depth) and a deep engineering geological (~ 170 m in deep) boring data have been utilized to investigate the Gölyaka basin (Fig. 4). The shallow boreholes utilized in this research were compiled from the Gölyaka Municipality and the State-Owned Development and Investment Bank (İlbank). They were drilled to conduct geological and geotechnical investigations for residential construction. The deep engineering borehole was drilled for hydrological investigation by the State Hydraulic Works (DSİ), a state funded agency under the Turkish Ministry of Environment and Forestry. The collected data were utilized to develop three profiles representing the basin margin of the northern and southern parts and the eastern section of the basin center (the deepest part). Based on the elaborated data,

Fig. 3 A view of the Gölyaka basin and Efteni lake from the south looking to the N-NE (**a**) and a close-up view of the lithological units and Quaternary alluvium from the study area. **b** Andesite of the Yığılca unit, **c** Sandstone outcrop of the Çaycuma formation at the margin of the basin, **d** sandy silty clay material, and **e** silty gravely sand material at the center of the basin

it was observed that groundwater was generally encountered at depths of 2.5 and 3.5 m from the surface, and it was situated almost at the surface towards the southeast of the study area.

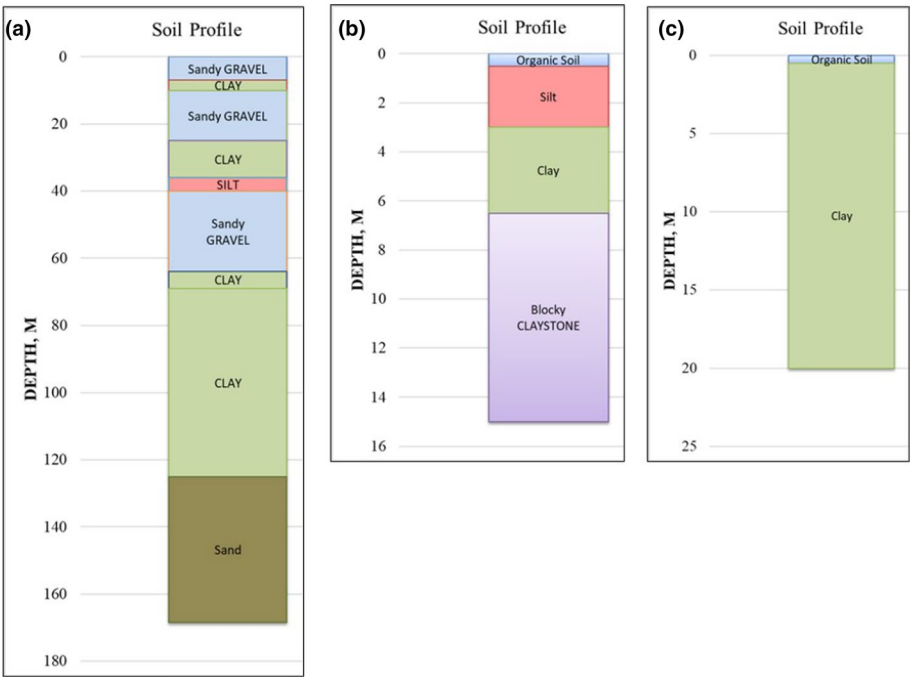

Fig. 4 A view of three representative soil profiles for the main boundary positions (**a** deep engineering geological boring profile at the deepest part of the basin, **b**, **c** geotechnical boring profiles at the northern and southern margin of the basin, respectively) (Yousefi-Bavil et al. 2018; Yousefi-Bavil 2022)

4.2 Surface wave methods

Field seismic measurements of active and passive surface wave methods have been conducted in the study area to obtain the shear wave velocity results. These techniques have been used jointly to maintain a reasonably high precision of shear wave velocity measurements not only at shallow depths but also at deeper sections (Park et al. 2007; Gosar et al. 2008; Koçkar et al. 2010; Eker et al. 2012; Koçkar and Akgün 2012; Gouveia et al. 2016; Koçkar 2016). An active source implies that the seismic energy is created with purpose at a particular location relative to the geophone array, and recording starts when the energy is conveyed into the ground (Park et al. 1999). On the other hand, in passive surface wave techniques (Okada and Suto 2003; Hayashi 2008), there is no time break, and therefore motion from ambient energy is created by a series of artificial sources (i.e., cultural noise, traffic, machinery, and so on) and natural phenomena (i.e., wind, wave motion) in different and often unknown locations according to the geophone array.

The primary difference between active and passive surface wave surveys in terms of outcomes is the different frequency ranges within which information can be gathered in such high-frequency components that are relatively easy to generate and detect in active testing. In contrast, microtremors are frequently very active in the low-frequency range. This approach is an extremely promising tool for subsurface research, as it enables soil

characterization to be extended to depths of tens or hundreds of meters. On the other hand, passive data are subject to more uncertainty, which, along with the intrinsic character of surface wave tests, results in lower resolution at depth. Additionally, the high-quality information associated with active data, along with the excellent resolution of surface waves at shallow depths, results in highly reliable results near the ground surface. With these constraints in mind, the dependability study demonstrated the necessity of combining active and passive data in order to provide more reliable and complete shear wave velocity data for engineering applications, particularly those requiring high resolution at shallow depths (Tokimatsu 1995; Rix et al. 2002; Yoon and Rix 2004; Park et al. 2005; Foti et al. 2007).

This study has mainly focused on high-resolution depths of 30 m and deeper depths, so the related configuration and instruments were selected accordingly. In order to obtain the subsurface Vs profile, multichannel analysis of surface wave (MASW) and microtremor array method (MAM) as active and passive surface wave methods have been conducted to measure the shear wave velocity down to great depths. It should be noted that the array design for both measured surface wave data was designed in a manner to optimize the complementarities of the collected frequency bands and to ensure an adequate overlap of the mutual frequency bands. As recommended in the literature, to measure the dispersion curve on the broadest possible frequency band, the concentric passive acquisitions have been applied from small to large spans (i.e., from 10 m up to 1 km or more depending on the targeted depth). As all dispersion curves were to be combined, active measurements were carried out near the center of the passive array, and finally, to prevent cross-contamination of the active and passive wave domains, simultaneous acquisition was avoided, as suggested by Foti et al. (2018).

In the Quaternary alluvium and terrace sediments, a total of 29 surface wave measurements that entailed both passive (MAM) and active (MASW) methods have been performed to characterize the sediments based on their age and depositional settings. The spatial distribution of the measurement points is presented in Fig. 2. In this part of the study, active MASW records with geophones spaced at 1.5 m with 5–10–15 m offset and a 16.5 m array length, and passive MAM records with geophones spaced at 5 m with 5 m offset and a 55 m length have been employed at each testing point. The field measurements were performed by adopting a grid system in which the seismic measurement points were placed approximately 700 m apart. However, this grid system had to be modified slightly during the fieldwork due to environmental noise, dense vegetation, and accessibility problems throughout the lake site and the infrastructures. It is believed that a combination of the distribution curves obtained by these active and passive methods results in obtaining a high-resolution sediment profile for seismic characterization (Eker et al. 2012; Koçkar 2016). The combined technique of the surface wave methods has been used to evaluate the underlying strata of the sediment profiles by using the Vs results.

A blind way technique was applied over the project site, and the primary purpose was to obtain the Vs profiles at the research site. The geophone type, offset length, and distance were selected accordingly to characterize the soil layers to a depth of at least 30 m or more. This method allowed correlating the results of both testing methods according to diverse sources. Even though some active source (MASW) measurements were affected by the far-field effect, the results verified that the effort put forward during the study produced highly satisfactory results. The latest models were developed by the presumption that the fundamental mode of Rayleigh-type surface wave was recorded in the wave analyses.

The processing and analysis of all MASW and MAM records acquired during the first and second phases were performed using the SeisImager/SWTM V. 2.2 Surface Wave

Analysis software. The same software was also used to combine active and passive SWMs at the same location. The phase shift (Park et al. 1999) and spatial autocorrelation (SPAC) inversion (Okada and Suto 2003) methods were utilized to obtain dispersion curves in the phase velocity frequency (v-f) domain for the MASW and MAM records, respectively. Figure 5 shows two examples of the constructed dispersion curves v-f domain for the MASW and MAM records.

Representative examples obtained from the processed dispersion curves were fit into the data and the Vs profiles from the active and passive surface wave measurements as presented in Fig. 6. Similar to Fig. 4, six profiles representing the basin margin of the southern

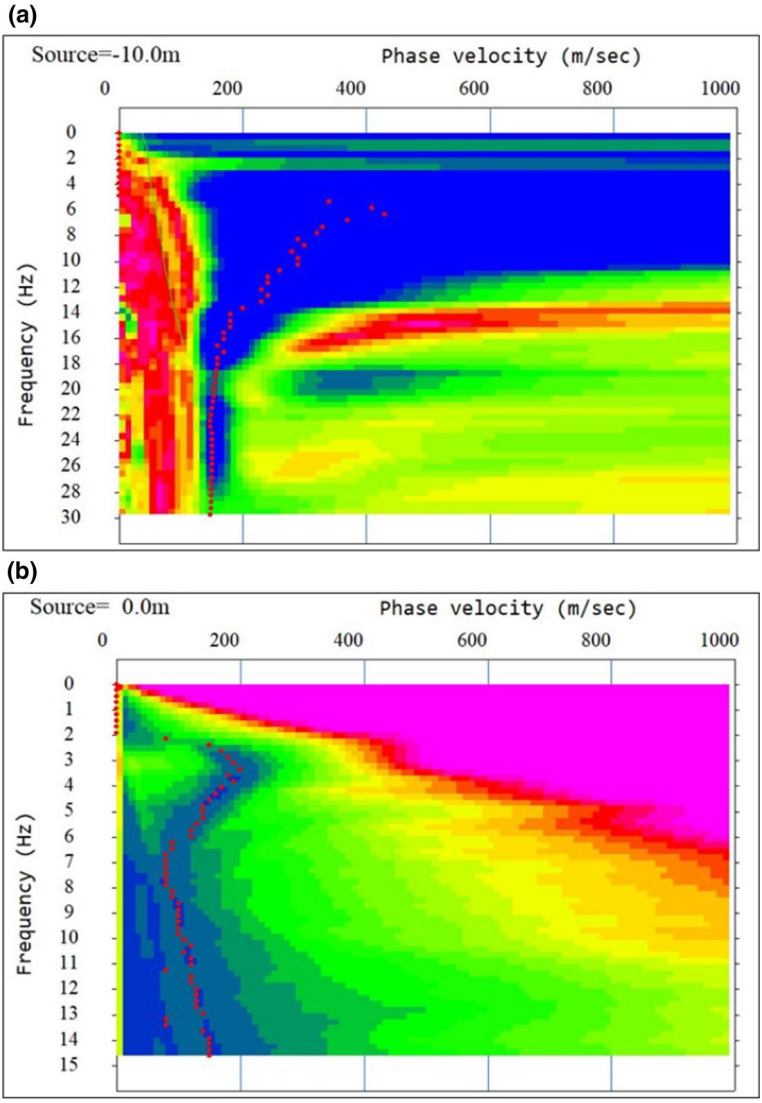

Fig. 5 Two examples of the dispersion curves of **a** Linear MASW and **b** linear MAM records at Seis-15

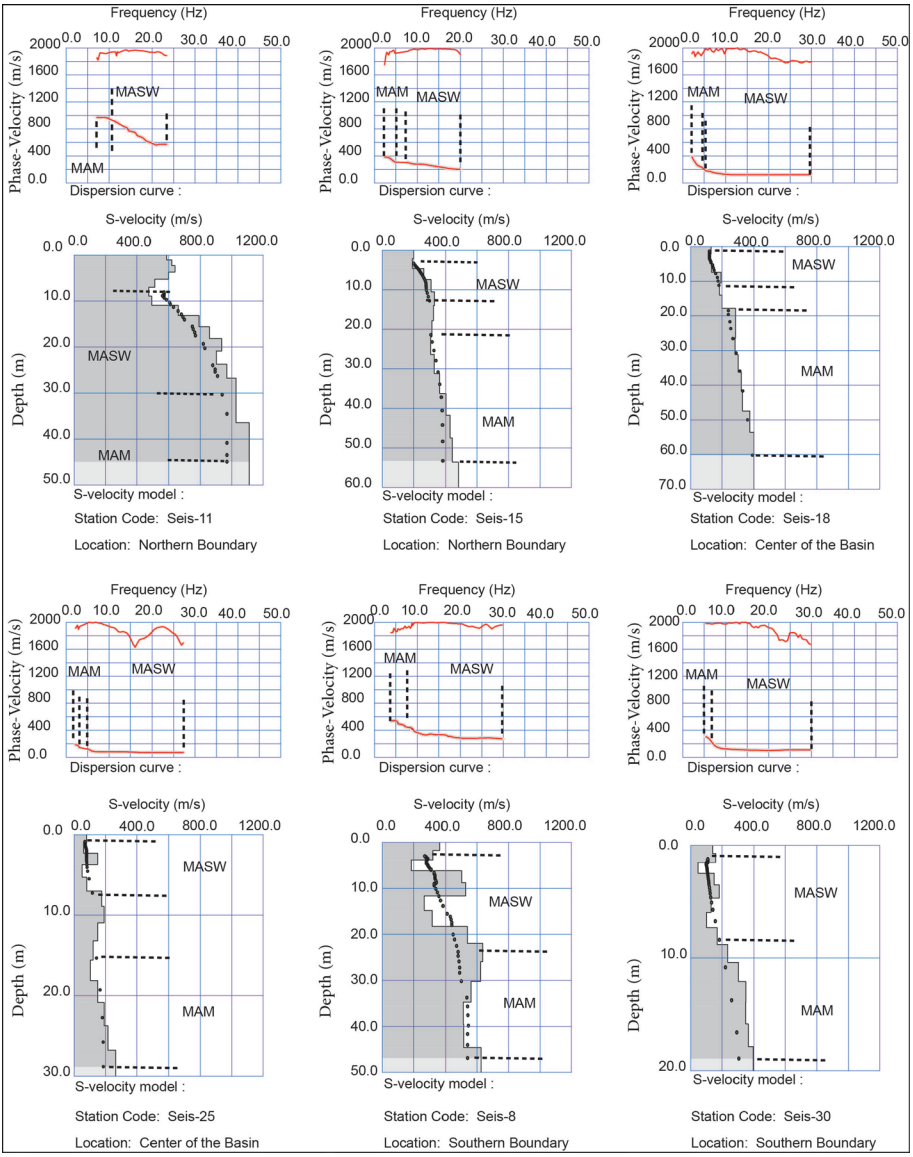

Fig. 6 Representative combined processed dispersion curves from MAM and MASW measurements and the corresponding Vs profiles with respect to the basin margin of the southern and northern parts along with the center of the basin

and northern parts and the center of the basin are presented in Fig. 6, where the consistency between these curves can be clearly seen. These results were also integrated and compared with the existing engineering geological and geotechnical boring data in the Gölyaka basin to confirm the validity of the conducted surface seismic testing results and thus aided in achieving more credible information on the subsurface sediments. With this procedure, the

quality of the data collected from the surface wave measurements was assessed, validated, and later, based on these results, the dimensional basin model of Vs was created.

Combining diverse datasets (surface wave measurements with different array spans) can supply an experimental dispersion curve over a wide frequency band. However, the branches of the dispersion curve in a variety of datasets must overlap with each other in the common frequency bands. A poor overlap might be related to various reasons (i.e., retrieval of different modes, lateral heterogeneity, lack of spectral resolution, difficulties in the processing step). In any event, an inadequate overlap confirms an analysis with poor reliability (Foti et al. 2018). In the Gölyaka basin, the combination of both methods has been thoroughly and accurately implemented, and representative examples extracted from different sections of the basin are given in Fig. 6.

4.3 Vertical electrical sounding (VES) method

The vertical electrical sounding (VES) method has become very popular in engineering investigations due to the simplicity of the technique. The VES method involves detecting surface effects produced by the flow of electric currents inside the earth (Telford et al. 1976). Vertical electrical sounding (VES) was carried out using the Schlumberger array at 14 stations in the study area. Since the overburden thickness of the basin was quite deep, it required long current electrode spacing for greater penetrations in such a way that the largest current electrode spacing AB/2 used was between 600 and 1250 m. The field survey encompassed vertical electrical sounding (VES) operations via the Schlumberger array (Takahashi 2004). Representative examples (from the measurement points G7 and G9) from the processed 1D profile of the VES measurements along with the inferred log details are presented in Fig. 7. It should be noted that the profile at point G7 illustrates a high resistivity value from the surface down to about 300 m below the surface due to the interference of the electrical conductivity of the gravelly and blocky sediments in the Quaternary alluvium unit.

4.4 H/V microtremor measurements

Several studies (Ibs-von Seht and Wohlenberg 1999; Özalaybey et al. 2011; Uebayashi et al. 2012; Eker et al. 2015) have shown that the resonance frequency obtained from microtremor measurements can be used to map the thickness of sediments. In this part of the study, some microtremor measurements were recorded using a single mobile station, and these records were processed by the H/V technique (Nakamura 1989) to verify basin depth and develop 2D Vs profiles. The spectral ratio between the horizontal and vertical components (H/V) of the microtremor measurements at the ground surface has been used to estimate the fundamental periods of the sites. The measurements were recorded with a Güralp model PC connected CMG-40TD seismograph with a frequency band ranging between 0.033 and 50 Hz with three component "servo type" velocity sensors. In this survey, data acquisition was performed by considering the SESAME procedures (SESAME 2004). The duration of the microtremor records was generally taken with 30 min of unprocessed waveform records and 100 Hz sampling interval. The seismograph was warmed up for 5 min at each location before recording microtremors for 30 min. The data quality (measurements) was simultaneously checked using a notebook PC during the recording process.

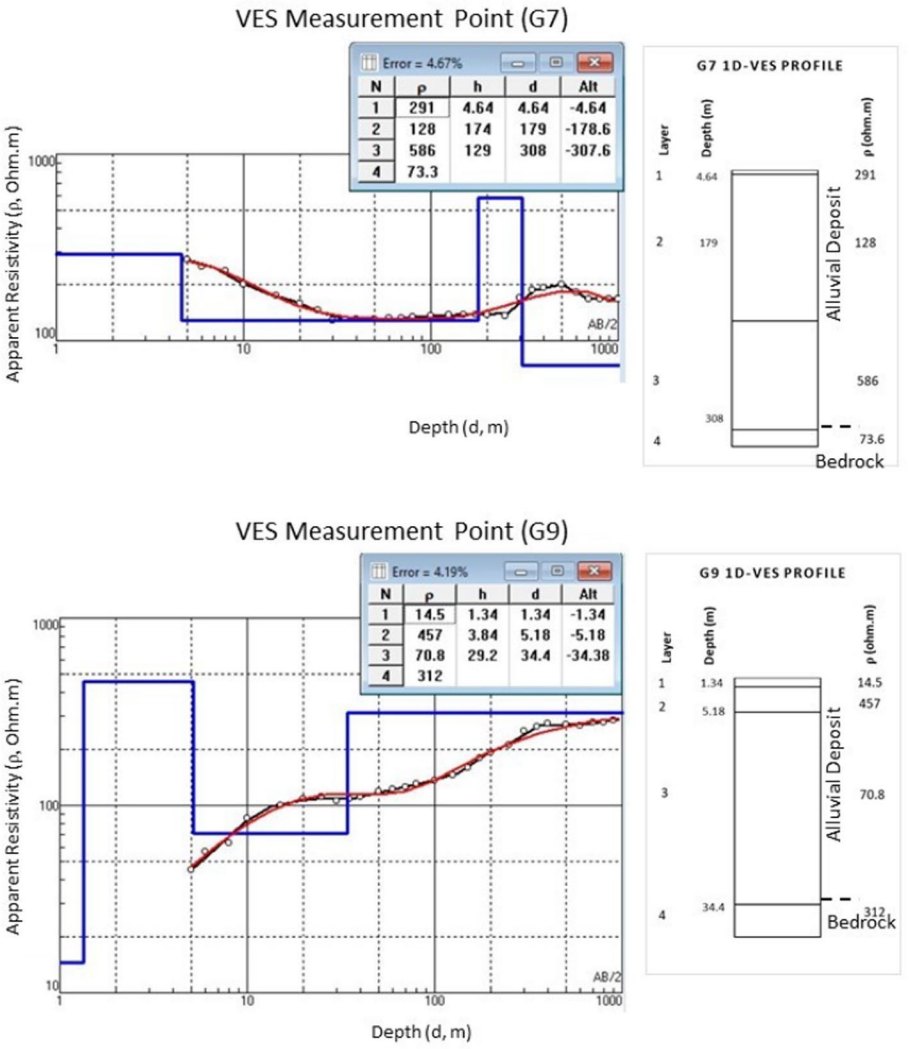

Fig. 7 Examples presenting the processed 1D profiles of vertical electrical sounding (VES) measurements along with their inferred log profiles in the study area (from the measurement points G7 and G9)

A fast Fourier transform (FFT) procedure was applied to each of these selected windows to waveform data (20 s) after period analysis during the data processing for each measurement point. Then the obtained Fourier spectrum was smoothened by applying the appropriate smoothing type and constant. Figure 8 illustrates the processed H/V results. The H/V spectral ratios were calculated at 0–10 Hz frequency intervals. The data indicated that the spectral ratio represented H/V curves with single, double, or broad peaks in the range of 0–10 Hz. Flat H/V curves were interpreted as "no-peak" values. Figure 8 shows the variation of the H/V spectral ratio curves obtained from the microtremor measurement points along with the Vs profile locations which will be discussed in detail in the later sections.

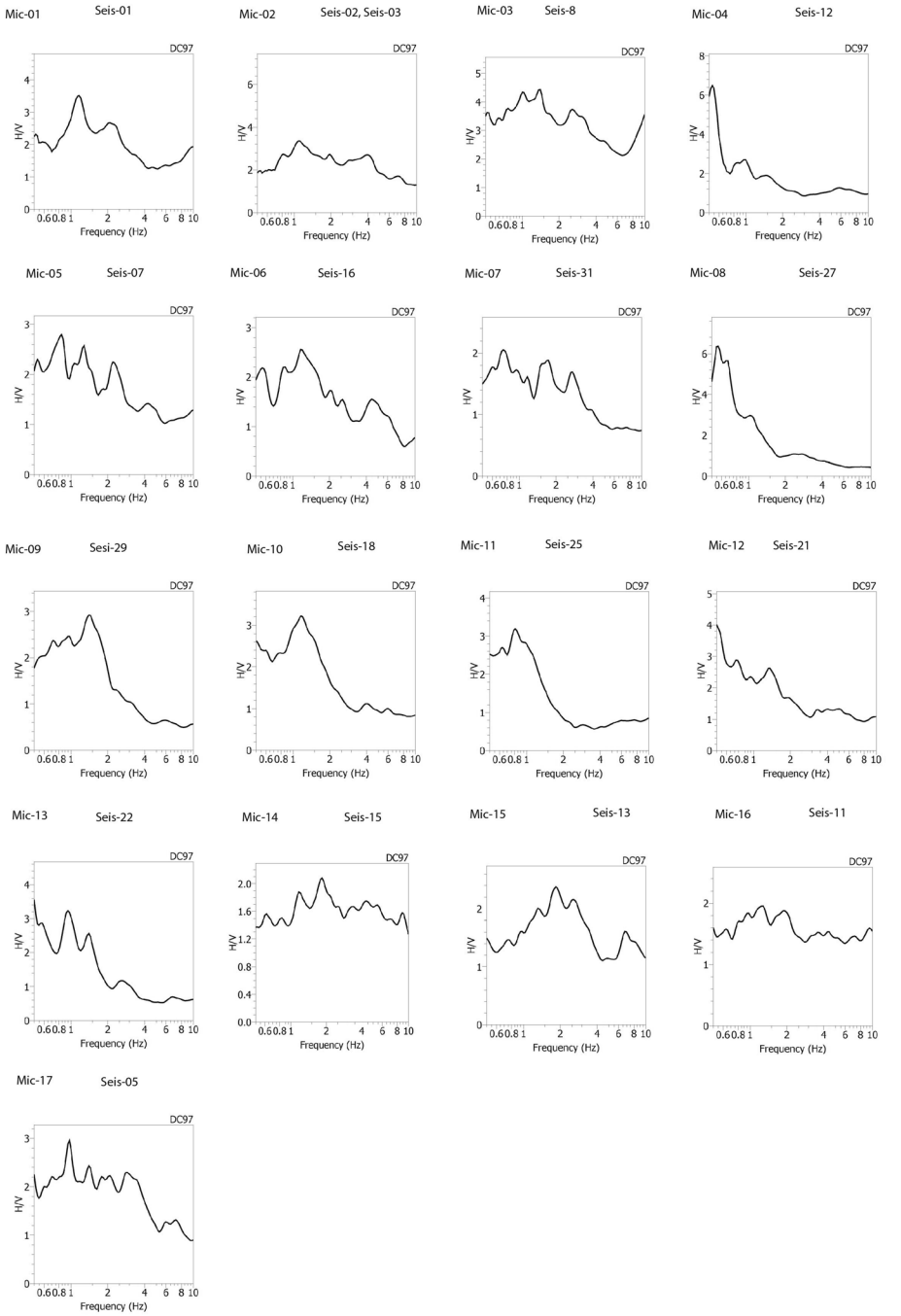

Fig. 8 The selected H/V spectral ratio curves in order to verify the given profile resulting from the measurements of the entire area. Note that seismic measurement points (i.e., Seis-01, -02) were indicated with the Vs profile locations which will be discussed in detail in later sections

5 Results

This section presents the results of the geotechnical and engineering geological boring and geophysical data (i.e., surface seismic testing, VES, and H/V microtremor measurements) along with the geology and topography of the basin to determine the presence of geological heterogeneities and the geometry of the basin in the Gölyaka region. A dimensional basin model has been developed based on these results.

The shallow geotechnical boring profiles along with the deep engineering geological boring profile (about 168.5 m) indicated that clay, gravel, silt, and sand-size sediments were present at shallow depths, whereas a thick layer of clay (about 61 m thick) was present in between 64 and 125 m (Figs. 2, 4). Finally, a sand layer about 43 m thick that underlies the clay layer reached down to a depth of 168 m. The laboratory index testing results obtained from the geotechnical boring data in the study area implied that the soil possessed low plasticity down to a depth of 15 m. According to the geotechnical laboratory data, the center of the basin was mainly composed of gravelly sandy silt and clay, and the clay content increased towards the northern boundary. At the same time, claystone was reached at a relatively shallow depth (i.e., at a depth less than 10 m), especially towards the northwestern part of the study area. From the deep engineering geological borehole data, it can be inferred that the thickness of the alluvial deposits increased significantly towards the east and the center of the basin, and this observation was consistent with the Vs profiles.

To prepare a well-developed basin model to define the topography and basin structure accurately, and thus to determine the spatial distribution both horizontally and vertically to evaluate the heterogeneity of the sediments, a 3D basin model has been developed in the tectonically active Gölyaka basin. The 3D basin model was developed with the aid of high-resolution Vs profiles obtained through surface wave methods using active MASW and passive MAM measurements (Fig. 9). Therefore, the vertical and horizontal variations of the shear wave velocity models have been developed to characterize the sedimentary units and differentiate the sediment type. While creating 3D Vs models, the basin was developed from 1D Vs profiles by utilizing a high-fidelity inverse distance weighting (IDW) method. Then, the upper surface boundary of the models was adapted according to the topography so that the digital elevation map (DEM) of the site was generated from the 1:25,000 topographic map of the HGK (the national mapping agency of Turkey under the Ministry of National Defense) and was later vertically exaggerated. The bottom surface of the models was extracted according to the Vs profile depths. In the development of the interpolated models, the combined results of the surface wave measurements of MASW and MAM measurements (i.e., Seis-01, -02) were used in conjunction with the vertical electrical sounding (VES) measurements and the deep engineering geological data to provide a well-developed basin geometry for the Gölyaka basin. Using the Vs results of 1100 m/s obtained from the shallow parts of the western boundary of the basin, the model was interpolated by considering the deep engineering geological borehole logs in terms of borings where the bedrock was not encountered down to a depth of about 260 m. According to the results of the VES measurements, the possible alluvial thickness was determined to be about 200–300 m, apart from the measurement taken at G7 which indicated a low apparent resistivity and hence a depth of almost 300–400 m. This anomaly could be attributed to the step-over faulting mechanisms of the Düzce fault segment or the presence of a bedrock formation of Eocene age (i.e., marl, claystone, or sandstone). Similar to the engineering geological boring data,

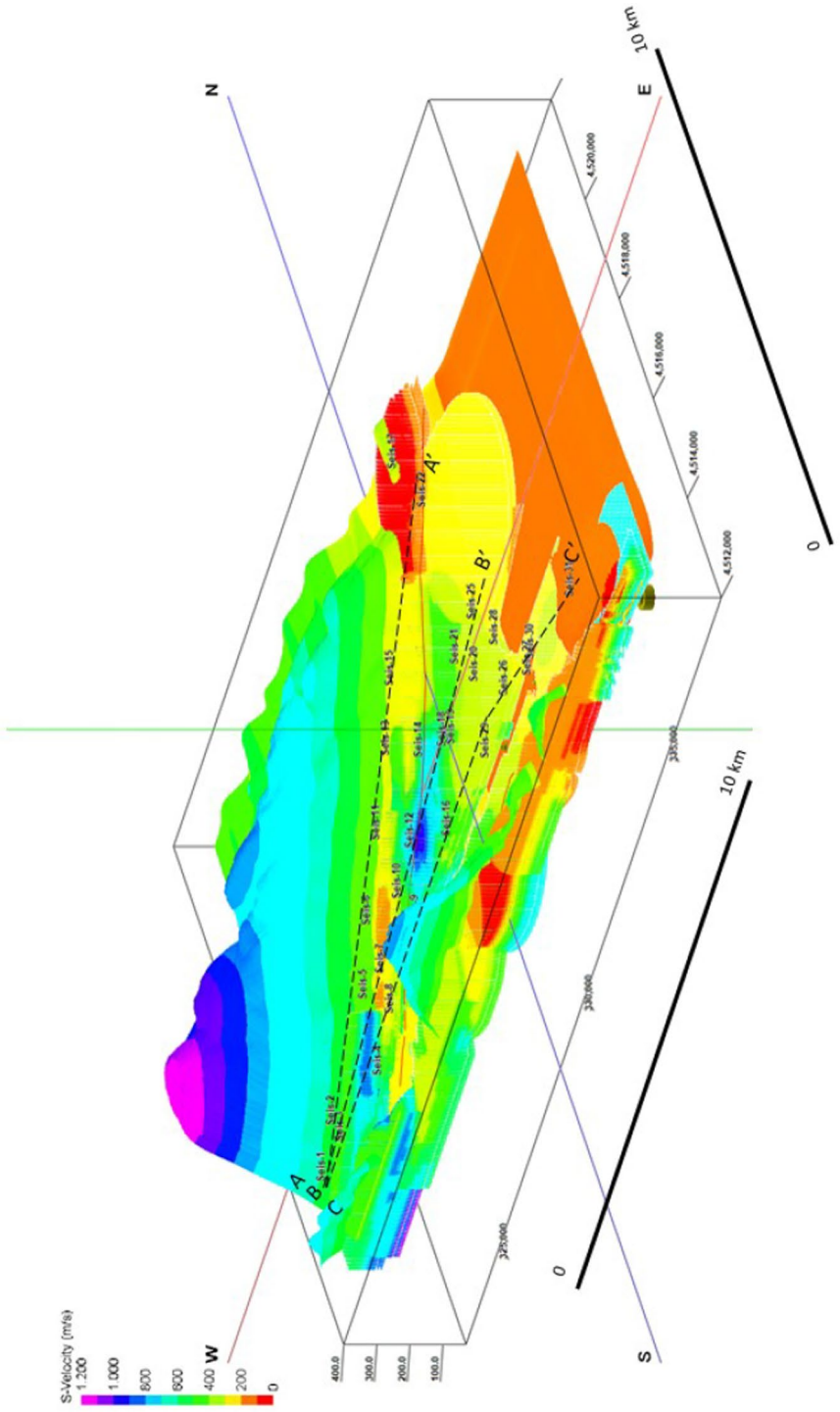

Fig. 9 A 3D basin model of the Vs results for the study area (vertical exaggeration: 5) (Yousefi-Bavil et al. 2018; Yousefi-Bavil 2022)

by the aid of the information obtained from the VES results, the Vs profile depths were comparatively interpolated down to the depth where an 1100 m/s shear wave velocity was attained (Fig. 9).

The results of the surface seismic measurements indicated that the shear wave velocities were less than 180 m/s in the upper 10–15 m of the Holocene alluvium or in the basin-ridge/terrace deposits. Shallow groundwater was suspected to exist owing to the Vs measurements of less than 150 m/s in both lithologies, as indicated by Yousefi-Bavil et al (2018). Considering the heterogeneity of the site, the surface seismic testing results were complemented by geotechnical and engineering geological deep boring studies and VES results (Yousefi-Bavil et al. 2018). The combined active and passive surface wave measurements determined in Plio-Quaternary sediments aided in constructing the 3D basin model (Fig. 9). As expected, the Vs results decreased as the thickness of alluvium increased towards the east. On the other hand, towards the west of the basin (i.e., towards the Upper-mid Eocene sedimentary deposits), the shear wave velocity increased since the depth of the bedrock decreased down to about 30–40 m, noting that in the engineering bedrock, shear wave velocity values greater than 1100 m/s were observed. It was further observed that the thickness of the engineering bedrock (i.e., approximately 200–250 m) was not encountered in the Vs profile at the basin where the valley expands. Therefore, the engineering bedrock was not observed in the middle of the basin (i.e., at a depth of about 50–100 m) due to the penetration of these sediments that bear lower shear wave velocity values to this particular depth. According to Dreger et al. (2007), at sites located near to a fault or within the low-velocity fault zone, the complexity of the surface seismic wave model in the form of velocity contrast with low velocity can be expected. The Vs results indicated that these conditions prevailed in the study area, especially near the faulting area at the southern edge and towards the southeastern part of the basin. Furthermore, these complexities in the velocity contrast were also observed in the center of the basin, where layers bearing lower Vs values were obtained in the middle of the section as stated previously (Yousefi-Bavil et al. 2018).

The VES results have also provided invaluable information to determine the thickness of the alluvial deposit and the depth of the engineering bedrock along with the faulting zone based on the geology and topography in the Gölyaka basin (Fig. 2). In addition, the results of this comprehensive survey were also used as complementary data for developing a well-developed 3D geometry of a basin model of the Gölyaka basin. The enlarged spatial distributions of the VES measurements and their profile locations (i.e., A1, A2, A3) used for preparing the cross sections are given in Fig. 1. Based on these results, a fence diagram given in Fig. 11 was developed from the VES measurements to prepare a 3D VES model obtained from the 1D VES profiles. This diagram illustrates the horizontal and vertical heterogeneity in both the N-S and E-W directions. In Fig. 11, it is observed that the thickness of the alluvial deposit varies considerably in the basin. The estimated maximum alluvial thickness is about 200–350 m in the center of the basin. As the resistivity increases from the center to the edge of the basin, the thickness of the alluvium decreases. Although the resistivity of the subsurface sediments is generally less than about 20 Ohm.m, the resistivity values of the bedrock (i.e., fractured sandstone/andesite) increase with depth (~ 200 Ohm.m) in the study area. In particular, the existence of near-field faulting and the geological observation can be clearly identified from the resistivity diagram in the measurement point of G10 as illustrated in the VES profiles (Fig. 10) and the fence diagram of the VES model (Fig. 11).

As illustrated in Fig. 11, an anomaly was observed towards the center of the basin where the G7 measurements were taken. Although the measured point indicated a high resistivity from the surface down to a depth of 300 m due to the presence of gravel and the blocky

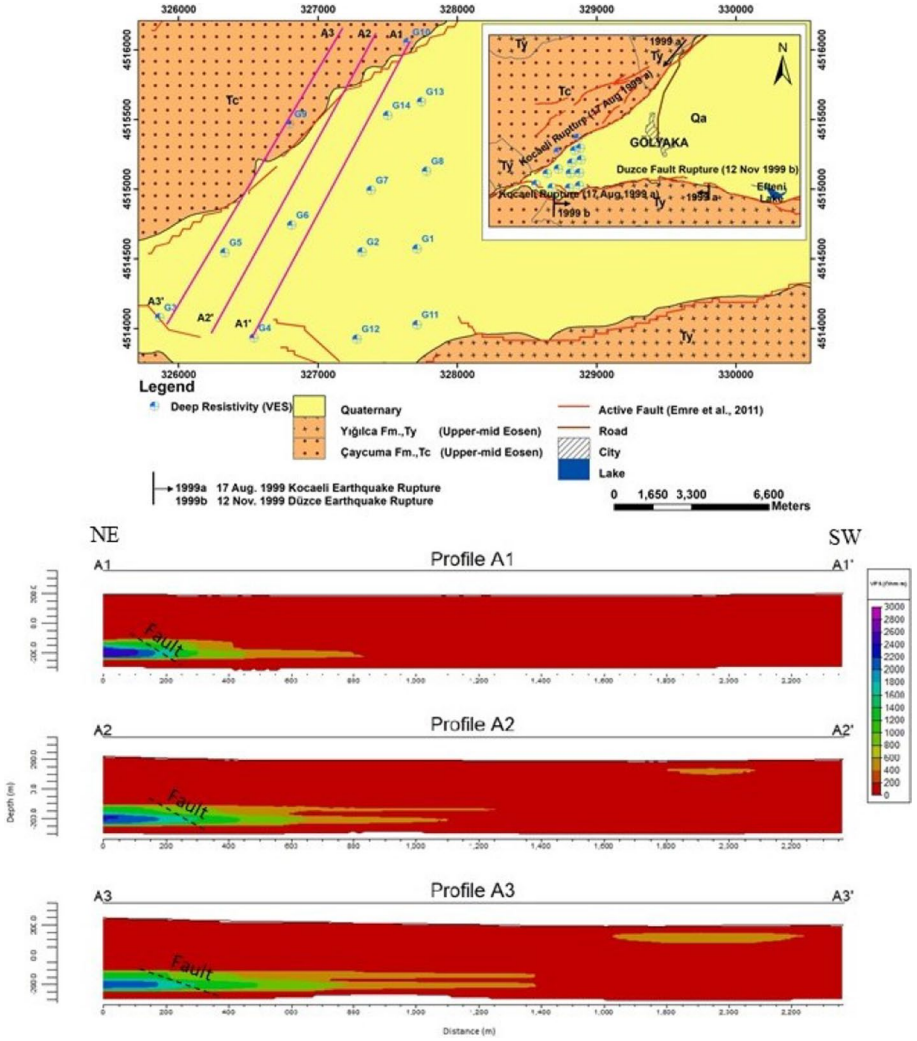

Fig. 10 Enlarged Fig. 2 showing the spatial distributions of the VES measurements, and three parallel profile locations (i.e., A1, A2, A3), It should be noted that the apparent resistivity contrast in the A1, A2, A3 points of the profiles are due to the zone of faulting (Modified from Yousefi-Bavil et al. 2018; Yousefi-Bavil 2022)

content of the Quaternary alluvium, a low resistivity layer was observed beyond this depth. Based on the surrounding VES measurements, faulting or Eocene age formation (i.e., marl, claystone, and sandstone) might be present at a depth beyond 300 m. Meanwhile, the Seis-7 measurement point, which is close to point G7, illustrates shear wave velocity values between 350 and 600 m/s down to a depth of 70 m, which is a good indicator for coarse material at this depth.

The H/V microtremor measurements taken in the study area were particularly used to verify the basin depth along with the developed 2D Vs profiles along the three sections in the Gölyaka basin (Fig. 9). Therefore, the variation of the H/V spectral ratio curves

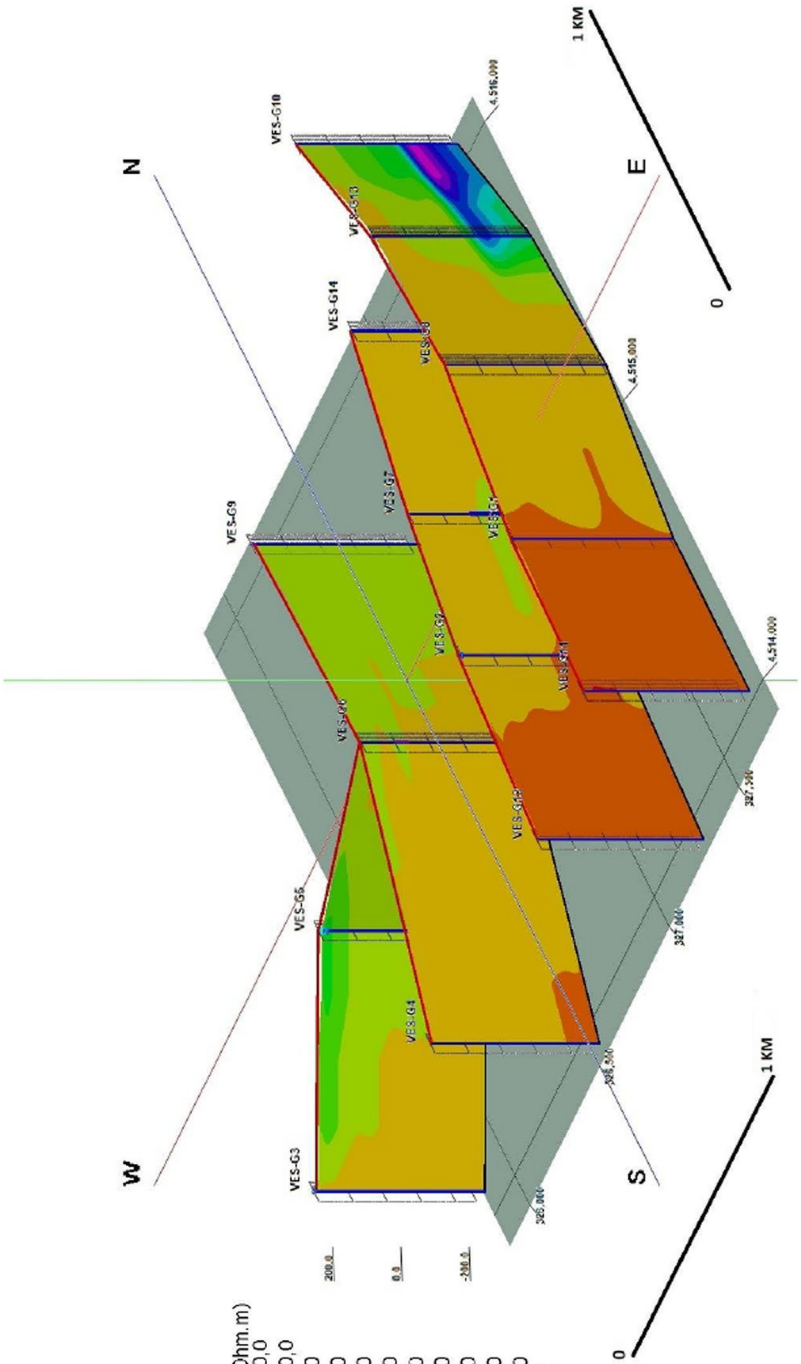

Fig. 11 A 3D fence diagram of the VES model. It should be noted that the apparent resistivity results decrease due to the zone of faulting in the northeast section (Yousefi-Bavil et al. 2018; Yousefi-Bavil 2022)

obtained from the microtremor measurement points shown in Fig. 8 as an example has been used to perform validation studies on the sections obtained from the Vs profiles. Also, these experimental data obtained by microtremor measurements were complementarily used in conjunction with the available engineering geological, geotechnical, and surface seismic test results to obtain reliable and comprehensive information from the H/V microtremor measurements based on fundamental frequencies in these areas. In this regard, the fundamental periods obtained from the microtremor measurements have been compared with the 2D Vs profiles throughout the developed cross sections presented in Fig. 12.

6 Discussion

A well-developed basin geometry that reflects a complex mechanism associated with the characteristics of the near-fault region could be accurately and reliably determined by developing a 3D basin model to assess site response. To this end, the developed 3D basin model based on the surface seismic testing results of Vs profiles is discussed in this section in relation to the geotechnical and geophysical test results that includes geology and basin topography. The H/V microtremor and VES testing results have been evaluated during the interpretation process to discuss and verify the inferred basin depth. The output of these comprehensive research studies to enable the construction of a well-developed 2D and 3D basin model in the Gölyaka basin is explained below.

Regarding the developed 3D basin model based on the Vs results (Fig. 9), the measurements indicated that the eastern and southeastern sides of the plain possessed lower Vs results. One of the possible reasons might be the shift of the course of the Efteni Lake from the east and the north to the southeast, where the Düzce faults and the present lake are situated. The presence of unconsolidated lacustrine sediments with variable thicknesses, horizontal variations in material properties, and their different consolidation degrees might be other reasons for observing different Vs results or velocity contrast in the basin center and at the edges (Yousefi-Bavil et al. 2018). Considering these facts, the Vs results were observed to be about 250–560 m/s and 150–360 m/s in the western and eastern parts of the basin, respectively, based on the coherency of the data. However, this coherency tended to become incoherent, particularly in the proximity of the fault.

The vertical and lateral variations of the Vs profiles across three sections were developed from the 3D basin model to characterize the sedimentary units and differentiate the sediment type. The trends of these sections are given in Fig. 12 as (a) the northern margin (along the 1999 Kocaeli fault rupture), (b) the basin center, and (c) the southern margin (along the 1999 Düzce fault rupture) of the Gölyaka basin. In preparation of the sections, the reliability of the results was ensured by taking sections along the route where the combined results of the MAM and MASW measurements in the study area were taken (i.e., Seis-01, -02). The thicknesses of the deposits according to the Vs values are given in each section. Section A–A′ (Fig. 12) passes through the northern boundary along the 1999 Kocaeli earthquake fault section, and especially the products of marginal depositional system can be easily determined with the help of the information along this section. The alignment of the C–C′ section that passes through the southern boundary along the 1999 Düzce earthquake fault section was selected to examine the variation in the shear wave velocity of the deposited sediments at different boundaries and lithological ages (Fig. 12). The B–B′ section that passes through the basin's center also provided information regarding the sedimentation systems that dominated the Quaternary period (Fig. 12).

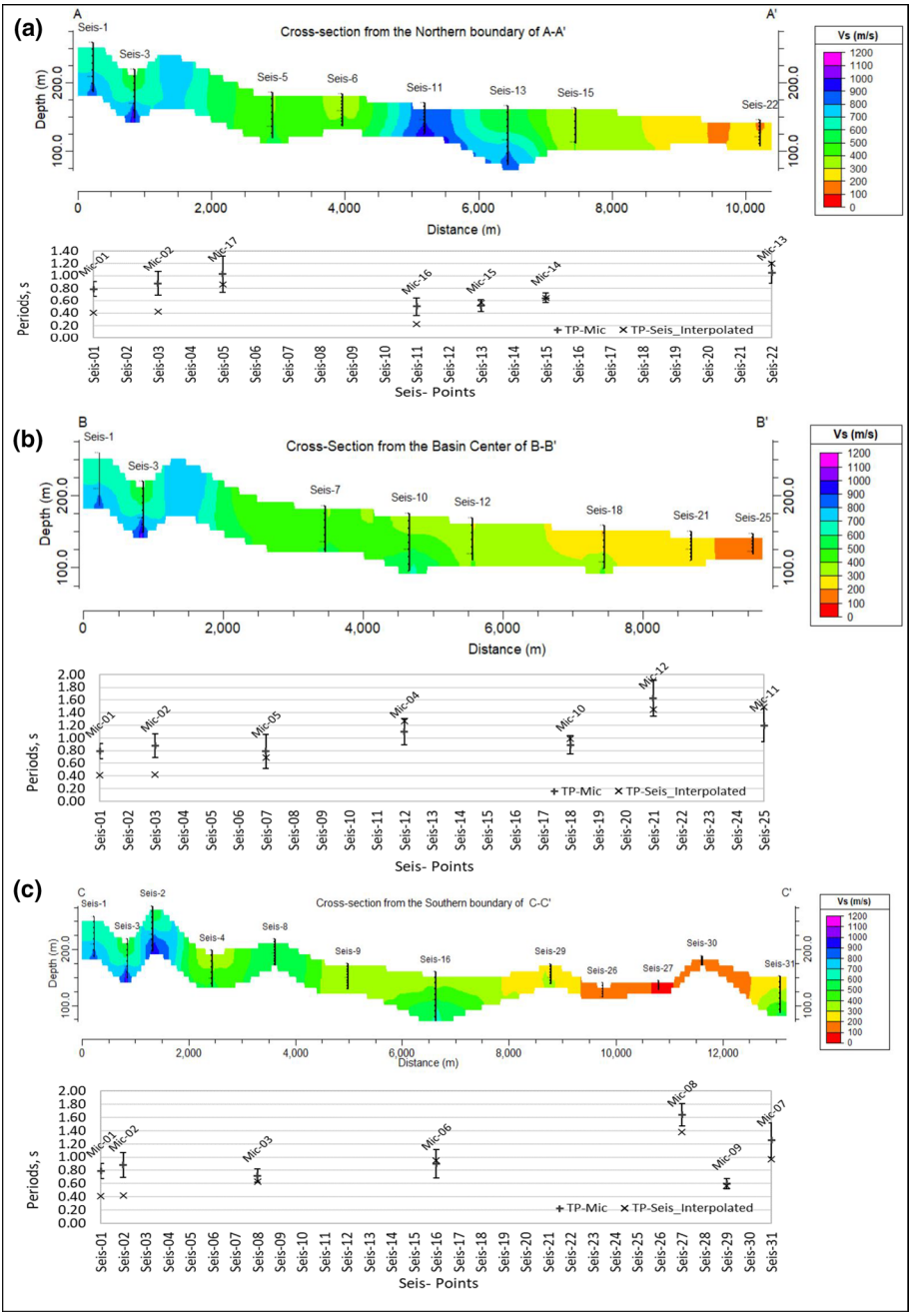

Fig. 12 A comparison of the three interpolated 2D cross sections of the Vs profiles along with the microtremor measurements that represent the northern (**a**) and southern (**b**) margins along with the basin center (**c**) of the Gölyaka basin (Vs profile vertical exaggeration: 10)

The middle of the depositional system, which is dominant at the side boundaries of the main course of the Büyükmelen River, consists of alluvial fan and terrace sediments deposited by debris flow. Because of the nature of the boundary depositional setting, the grain size of the sediments is larger than those located on the southern side and those that are present towards the eastern sedimentation system that consists of fine-grained alluvial plain sediments such as sand, silt and clay. Thus, the Vs results of the marginal depositional system are higher than those at the center. The Vs profiles of the models at the Seis-20, Seis-25 sites are located at the Büyükmelen river course, where it migrates towards the north of the region (Fig. 12b). Examining the Vs profiles of these measurement points (i.e., considering that all sections were taken along the measurement locations of the study area), it was observed that the layers with coarse-grained materials having high shear wave velocity displayed lateral transition into layers of fine-grained materials having relatively low-velocity results due to the heterogeneity of the alluvial deposits.

The saturation of the sediments due to the presence of the course of the Efteni lake towards the south has also contributed to this phenomenon. The reason for these lateral transitions could have been either due to a wedge-type topography, near-field faulting, or stratification based on the depositional setting that controls the depositional environment, namely the shear zone or the braided river system. In addition, the shear zone due to faulting could be observed in the two sections that pass through the northern and the southern boundary on Seis-11, Seis-26, Seis-27, and Seis-30 (Fig. 12a, c). It should be noted that the heterogeneity in the measurements along both sections could be attributed to the deformation created by faulting, which implied that stiffer material was sitting next to the softer and saturated soil or vice versa. In other words, these sediments represented themselves as low shear wave velocity sediments (< 180 m/s) bordering higher velocity sediments (> 500 m/s).

Regarding the 3D fence diagram of the VES model, examining the VES locations G13, G8, and G1 at the east of the diagram indicates that the higher resistivity results start from the surface and continue down to 200–350 m because the presence of coarse-grained materials have prevented electrical conductivity in the Quaternary unit. It is strongly believed that the progression in the lower resistivity layers is due to the transition to the Eocene-aged units in these layers (i.e., marl, mudstone, sandstone). The VES point of G9 at the northern part of the diagram presents highly variable resistivity values as it progresses over the Quaternary unit at shallower depths (i.e., at a depth of 35 m). The higher resistivity value (312 Ohm.m) after 35 m suggests that it has entered into the Yığılca unit (i.e., andesite, basalt), which can be accepted as bedrock. Likewise, the decrease in resistivity after 140 m at the VES point of G6 most probably indicates a fault between points G9 and G6. The VES points of G4, G11, and G12, which are in the same direction of the Düzce Fault, remained in the south of the diagram. An anomaly observed at the VES point of G4 may indicate a different unit with high resistivity. The increased resistivity with depth in the VES measurements of G11 and G12 most probably indicates that bedrock was encountered at a shallower depth and progressed into this unit.

As mentioned in the previous section, during the development of the 3D basin model, the surface seismic measurements have been analyzed and processed comparatively with the VES measurements and the deep engineering geological results to provide a well-developed basin geometry of the Gölyaka basin. Then, by the aid of the information obtained from the VES results, the Vs profile depths were interpolated with depth through considering the bedrock geometry. Regarding this procedure, it needs to be mentioned that while the depths of the observed Vs profiles are about 70–90 m at the most, the deep VES measurements covered a depth of more than 300 m. Therefore, deep VES surveying results

have been complementary to the depth-related processing of the shear wave velocity profiles conducted in the study area to observe the vertical and horizontal heterogeneity of the basin. This method enabled the detection of faults at the measurement point G10 in the profiles as illustrated in Fig. 11. Furthermore, the possible bedrock depth and/or possible faulting due to the over-step mechanism of the Düzce fault observed at the measurement point G7 is also presented in Fig. 11. As a result, it can be inferred from the deep VES results that the results provided invaluable information to estimate the thickness of the alluvial deposit through the bedrock and to evaluate the lateral variation of the basin complexity in the tectonically active near-fault region. Then, these results were used complementarily to develop a 3D geometry of the basin model of the Gölyaka basin.

Considering the cross sections of the Vs profiles along with the microtremor measurements, section A-A′ in Fig. 12a runs through the northern boundary of the basin where the bedrock depth is just beneath the sediments that are a few meters thick towards the west of the profile. As seen in the profile at Seis-1 and 3, Vs values of about 1100 m/s were obtained, and the bedrock depth is quite shallow. At these two points, the predominant periods calculated from the Vs profiles ($T_p \sim 0.41$) having shallow bedrock thicknesses by using the quarter-wavelength method ($T_p = 4H/V_s$) were not concordant with the fundamental periods measured by the H/V microtremor survey at points Mic-01 ($T_p \sim 0.79$ s $\pm 1\sigma$) and Mic-02 ($T_p \sim 0.88$ s $\pm 1\sigma$), which gave relatively higher anomaly results. In addition, the fundamental period measured at the Mic-16 measurement point ($T_p \sim 0.51$ s $\pm 1\sigma$) inferred higher period values than those calculated from the Vs profile of Seis-11 ($T_p \sim 0.2$ s) while the fundamental period measured at the Mic-14 measurement point (T_p 0.65 s 1) inferred the same period values as those calculated from the Seis-15 Vs profile (T_p 0.65 s). All these results are probably due to the non-linear behavior of soils, such as shallow bedrock depth (impedance contrast), material deformation (velocity contrast), and basin edge effects. In addition to these results, thicker sediment deposits led to higher fundamental periods towards the center of the basin from the northern border, as clearly observed in Mic-13. Here, the predominant period calculated from the Seis-22 Vs profile of the 3D basin model of ($T_p \sim 1.2$ s) was consistent with the measured H/V results from microtremors. This result verified the estimated thickness of the 3D basin model at this location. In Fig. 12b, section B–B′ runs through the center of the basin, where the deposit thickness or basin depth increases rapidly from the west towards the center. Here, the bedrock depth rises significantly from about 60 m at points Seis-01 and 03, to about 170 m at point Seis-07, and to about 250–300 m at points Seis-10, 12, 18, 21, and Seis-25, respectively. At the sites where the estimated bedrock is present at a depth of more than 250–300 m (i.e., the location of microtremor measurement points of Mic-04, 10, 11, and 12 at the center of the basin) around the Gölyaka basin with thicker deposits, the fundamental period took on relatively higher values as compared to those at the edge of the basin ($T_p \sim 1$ to 1.7 s) (Fig. 8). The predominant period calculated from the Vs profiles of Seis-21 ($T_p \sim 1.45$ s) was well suited within the lower limit of the period as estimated from the microtremor results of Mic-12 ($T_p \sim 1.63$ s $\pm 1\sigma$). Similarly, at Mic-10, 11, 12 towards the east of the basin where the thicker deposits exist, the higher fundamental periods (1.1–1.7 s) observed verified the estimated bedrock depth. Section C–C′ in Fig. 12c cuts through the southern boundary of the basin along the Düzce fault rupture. Since the trend of this cross section was not a straight line, the bedrock depth increased drastically from about 70–90 m along the southern boundary to about 200 m at a distance of just a few tens of meters from the basin edge at the measurement point Seis-27. The rapid deepening of the bedrock at this point has inferred the presence of faulting with a sharp dip. Comparing the fundamental period results obtained from microtremor measurements (Mic-08; $T_p \sim 1.64$ s $\pm 1\sigma$) with the

predominant period results obtained from the Vs profiles ($T_p \sim 1.38$ s) that depend on the interpolated data from the basin model verified the estimated deep bedrock. In summary, these high predominant period results are most likely due to the thick unconsolidated and soft sediments of the Efteni lake deposits and the tectonic activity-related deformation that controls these deposits. In general, the determined fundamental periods from the microtremor measurements with one standard deviation ($T_p \sim 0.6$ to 1.2 s $\pm 1\sigma$) at points Mic-03, 06, 07, 09 are consistent with the predominant periods estimated from the Vs profiles in the basin at points Seis-8, 16, 29, 31. Hence, these results confirm the estimation of the bedrock depth of the basin model at these locations (about 70–90 m).

As a result of the evaluation of three sections taken from the basin, it has been observed that there is no inconsistency between the dominant period values obtained by seismic measurements at the basin edge, where the bedrock depth is known, and the dominant period values measured directly by the microtremor method. These results are consistent with the basin edge effects observed at the basin's boundary, where a distinct impedance contrast between the layers is observed. Notably, they do not affect the estimated basin depth due to the non-linear topography and heterogeneity along the active fault zone. On the other hand, although the estimated basin depth at the basin center was not precisely known, the predominant periods estimated by the interpolated results from the basin model have proven to be consistent with the data obtained by the microtremor measurements. These results confirm the suitability of the microtremor method as complementary along with the other aforementioned methods used in determining the bedrock depth model and for developing a well-developed 3D geometry of a basin model of the Gölyaka basin.

7 Summary and conclusions

This study has assessed the local site conditions along with the sediment characteristics in the Gölyaka basin, which tends to possess complex geology because of tectonic deformation caused by near-field faulting. The inclination of a layer and lateral heterogeneity caused by material deformation can be significant due to its proximity to faulting. A 3D basin model was developed to characterize the sedimentary layers based on the 1D Vs profiles obtained from both active and passive surface wave methods that provided a high resolution of the Vs profiles for shallow depths. In addition, the Vs profiles were correlated with the deep VES results, geology, and available geotechnical boring data. These data allowed to check the validity of the basin model based on surface wave velocity results in the corresponding layers.

Based on the shear wave velocity results, 1100 m/s was accepted as the bedrock depth limit in the region. Furthermore, the results suggested that the Gölyaka basin was primarily composed of thick clay and sand deposits with some lenses of gravel sediments and with the transition between these layers. The results of this study illustrated that the calculated Vs values with depth implied the prevalence of a low-velocity zone in some pocket areas, especially in the near-field of the fault rupture zone and the saturated lake deposits in the southern boundary. Furthermore, these complexities in the velocity contrast were observed in the center of the basin, where the sediment layers with lower Vs values were determined in the mid-depth of the basin (i.e., at a depth of 50–100 m). The extracted 2D shear wave velocity profiles illustrated that the thickness of the basin sediment continued down to a depth of approximately 250–350 m with irregular geometry due to over-step faulting near the southern boundary of the basin. As

a result, the local site conditions have demonstrated spatial variations in the near-field area depending on the dimensional basin geometry, material heterogeneity, and topography. As a result, inclined layering and nonlinearity in the Vs profiles have formed. The lateral heterogeneity and incoherence in the Vs measurements were not so dominant in the developed Vs-model but were rather dominant in the near field of the fault zone, where the low-velocity material sits next to the higher velocity material. The surface seismic survey results were complemented with the deep vertical electrical sounding (VES) measurements, the engineering geological, and geotechnical data along with the geology to increase the authenticity of the research reported herein.

In the VES results, the lateral variation of basin complexity due to the heterogeneity of the near-fault region was observed. An increase in the thickness of the alluvium in the center of the basin indicates that the alluvium could be much thicker, i.e., almost 450 m. Nevertheless, these results can also be attributed to the transition zones between the deformed material due to the near-field fault activity and thus the tectonic deformation of the rock formations. In addition, the existence of faulting could also be observed throughout the resistivity results that were in good agreement with the geological and topographical observations.

The H/V microtremor measurement verified the estimated basin depth at the Gölyaka region. The correlation between the measured fundamental periods of H/V and estimated Vs profiles presented a good agreement, especially at the center of the basin. Inconsistent results have been occasionally observed along the Kocaeli and Düzce fault ruptures in the northern and southern boundaries due to basin edge effects and tectonic deformation of the materials. Additionally, at the western side of the basin, where the bedrock depth is shallow, impedance contrast was observed between these layers, which was also validated by the H/V microtremor results.

This study is a pioneer study for a highly seismically active region in the near-fault sites, such as the Gölyaka basin, concerning the initial evaluation of site response analysis in an account for seismic hazard assessment. It is vital to have an appropriate well-developed basin model for seismic hazard evaluations, general land use, and urban planning for such a large district with growth potential in a near-fault region, while it experiences a major earthquake. In conclusion, it is strongly believed that the model developed in this study can be reliably utilized to evaluate site effects and site response studies in the near-field region. After that, additional site-specific studies could be performed in this unique basin to more accurately describe the characteristics and potential level of ground shaking in seismic hazard assessment. This study is believed to form an excellent example of why the advanced basin model should address the complexity associated with the characteristics of the near-fault region, which is yet not fully understood as related to the effects of major seismic events.

Supplementary Information The online version contains supplementary material available at https://doi.org/10.1007/s11069-022-05418-4.

Acknowledgements The authors would like to thank the Middle East Technical University (METU) Scientific Research Project (BAP-03-09-2012-002) for providing financial support for this study. The authors thank the anonymous reviewers for their constructive comments and Dr. Margaret Sönmez for comments on the use of language. It should be pointed out that some parts in the "Seismotectonics and seismicity" section, as well as in the "Conclusions and discussion" section, have some similarities with a conference paper of the same author(s) that is cited in the link below: http://papers.16ecee.org/files/16ECEE%20FullPaper%20Thessaloiki.pdf. The authors appreciate the assistance of Ms. Arzu Arslan Kelam, Research Assistant, Department of Geological Engineering, Middle East Technical University (METU) during the fieldwork.

Funding The research performed in this study was supported by the University Research Project No. BAP-03-09-2012-002, which the third author (Haluk Akgün) has received from the Middle East Technical University (METU) Research Fund.

Declarations

Conflict of interest The authors declare no conflicts of interest.

References

Ajala R, Persaud P (2021) Effect of merging multiscale models on seismic wavefield predictions near the southern San Andreas fault. J Geophys Res: Solid Earth 126:e2021JB021915. https://doi.org/10.1029/2021JB021915

Akyüz HS, Hartleb R, Barka A, Altunel E, Sunal G, Meyer B, Armijo R (2002) Surface rupture and slip distribution of the 12 November 1999 Düzce earthquake (M 7.1), North Anatolian fault, Bolu, Turkey. Bull Seismol Soc Am 92(6):1–6. https://doi.org/10.1785/0120000840

Ambraseys NN, Zatopek A (1969) Mudurnu Valley, West Anatolia, Turkey, Earthquake of 22 July 1967. Bull Seismol Soc Am 59:21–89

Aydan Ö, Ulusay R, Kumsar H, Tuncay E (2000) Site investigation and engineering evaluation of Düzce-Bolu earthquake of November 12, 1999, Turkish Earthquake Foundation (TDV), 220 p

Bakir PG, De Roeck G, Degrande G, Reynders E (2007) Seismic demands and analysis of site effects in the Marmara region during the 1999 Kocaeli earthquake. Nat Hazards 42:169–191. https://doi.org/10.1007/s11069-006-9067-0

Barka A (1996) Slip distribution along the North Anatolian fault associated with the large earthquakes of the period 1939 to 1967. Bull Seismol Soc Am 86(5):1238–1254. https://doi.org/10.1785/BSSA0860051238

Barka AA, Kadinsky-Cade K (1988) Strike-slip fault geometry in Turkey and its influence on earthquake activity. Tectonics 7(6):63–84. https://doi.org/10.1029/TC007i003p00663

Barka A, Akyüz HS, Altunel E, Sunal G, Çakir Z, Dikbas A, Yerli B, Armijo R, Meyer B, De Chabalier JB, Rockwell T, Dolan JR, Hartleb R, Dawson T, Christofferson S, Tucker A, Fumal T, Langridge R, Stenner H, Lettis W, Bachhuber J, Page W (2002) The surface rupture and slip distribution of the 17 August 1999 İzmit earthquake (M 7.4), North Anatolian fault. Bull Seismol Soc Am 92(1):43–60. https://doi.org/10.1785/0120000841

Biswas R, Baruah S, Bora N (2018) Assessing shear wave velocity profiles using multiple passive techniques of Shillong region of northeast India. Nat Hazards 94:1023–1041. https://doi.org/10.1007/s11069-018-3453-2

Boaga J, Vaccari F, Panza GF (2010) Shear wave structural models of Venice Plain, Italy, from time cross correlation of seismic noise. Eng Geol 116:189–195. https://doi.org/10.1016/j.enggeo.2010.09.001

Borcherdt RD (2002) Empirical evidence for acceleration-dependent amplification factors. Bull Seismol Soc Am 92:761–782. https://doi.org/10.1785/0120010170

Bradley BA, Cubrinovski M (2011) Near-source strong ground motions observed in the 22 February 2011 Christchurch earthquake. Seismol Res Lett 82:853–865. https://doi.org/10.1785/gssrl.82.6.853

Bürgmann R, Ayhan ME, Fielding EJ, Wright TJ, McClusky S, Aktug B, Demir C, Lenk O, Türkezer A (2002) Deformation during the 12 November 1999 Düzce, Turkey, earthquake, from GPS and InSAR data. Bull Seismol Soc Am 92(1):161–171. https://doi.org/10.1785/0120000834

Cambazoğlu S, Koçkar MK, Akgün H (2016) A generalized seismic source model for the Eastern Marmara Region along the segments of the North Anatolian Fault System. Soil Dyn Earthq Eng 88:412–426. https://doi.org/10.1016/j.soildyn.2016.07.002

Cushing EM, Hollender F, Moiriat D, Guyonnet-Benaize C, Theodoulidis N, Pons-Branchu E, Sépulcre S, Bard PY, Cornou C, Dechamp A, Mariscal A, Roumelioti Z (2020) Building a three dimensional model of the active Plio-Quaternary basin of Argostoli (Cephalonia Island, Greece): an integrated geophysical and geological approach. Eng Geol. https://doi.org/10.1016/j.enggeo.2019.105441

Dobry R, Borcherdt RD, Crouse CB, Idriss IM, Joyner WB, Martin GR, Power MS, Rinne EE, Seed RB (2000) New site coefficients and site classification system used in recent building seismic code provisions. Earthq Spectra 16:41–67

Dreger DS, Transportation CD, University of California, B.E.E.R.C. (2007) Near-fault seismic ground motions. UCB/EERC 2007-03. California

Eker AM, Akgün H, Koçkar MK (2012) Local site characterization and seismic zonation study by utilizing active and passive surface wave methods: a case study for the northern side of Ankara, Turkey. Eng Geol 151:64–81. https://doi.org/10.1016/j.enggeo.2012.09.002

Eker AM, Koçkar MK, Akgün H (2015) Evaluation of site effect within the tectonic basin in the northern side of Ankara. Eng Geol 192:76–91. https://doi.org/10.1016/j.enggeo.2015.03.015

Emre Ö, Doğan A, Duman TY, Özalp T (2011) 1:250.000 Scale Active Fault Map Series of Turkey. General Directorate of Mineral Research and Exploration Ankara- Turkey

Foti S, Comina C, Boiero D (2007) Reliability of combined active and passive surface wave methods. Rivista Italiana di Geotecnica 41(2):39–47

Foti S, Hollender F, Garofalo F, Albarello D, Asten M, Bard PY, Comina C, Cornou C, Cox B, Di Giulio G, Forbriger T, Hayashi K, Lunedei E, Martin A, Mercerat D, Ohrnberger M, Poggi V, Renalier F, Sicilia D, Socco V (2018) Guidelines for the good practice of surface wave analysis: a product of the InterPACIFIC project. Bull Earthq Eng. https://doi.org/10.1007/s10518-017-0206-7

Gazetas G, Kallou PV, Psarropoulos PN (2002) Topography and soil effects in the MS 5.9 Parnitha (Athens) earthquake: the case of Adámes. Nat Hazards 27:133–169. https://doi.org/10.1023/A:1019937106428

Gosar A, Stopar R, Rošer J (2008) Comparative test of active and passive multichannel analysis of surface waves (MASW) methods and microtremor HVSR method Primerjalni test aktivne in pasivne večkanalne analize površinskih valov (MASW) ter metode mikrotremorjev (HVSR). Mater Geoenvironment 55:41–66

Gouveia F, Lopes I, Gomes RC (2016) Deeper VS profile from joint analysis of Rayleigh wave data. Eng Geol 202:85–98. https://doi.org/10.1016/j.enggeo.2016.01.006

Gürer Ö, Sangu E, Özburan M (2006) Neotectonics of the SW Marmara region, NW Anatolia. Turkey. Geol Mag 143(2):229–241. https://doi.org/10.1017/S0016756805001469

Hayashi K (2008) Development of the surface-wave methods and its application to site investigations. Kyoto Univ. Dr. Diss. https://doi.org/10.14989/doctor.k13774

Herak M (2008) Model HVSR-A Matlab® tool to model horizontal-to-vertical spectral ratio of ambient noise. Comput Geosci. https://doi.org/10.1016/j.cageo.2007.07.009

Ibs-von Seht M, Wohlenberg J (1999) Microtremor measurements used to map thickness ofsoft sediments. Bull Seism Soc Am 89(1):250–259

Joyner WB, Fumal TE, Glassmoyer G (1994) Empirical spectral response ratios for strong motion data from the 1989 Loma Prieta, California, earthquake. In: NCEER-94-SP01, R.S.P. (ed) Proceedings of 1992 NCEER/SEAOC/BSSC workshop on site response during earthquake and seismic code provisions. National Center for Earthquake Engineering Research, Buffalo, NY, Los Angeles, California, G.R. Martin (ed)

Koçkar MK (2016) Site characterization of the strong motion stations and evaluation of site effects in the Ankara region during the December 2007 and March 2008 moderate Bala earthquakes. Environ Earth Sci. https://doi.org/10.1007/s12665-016-5921-x

Koçkar MK, Akgün H (2012) Evaluation of the site effects of the Ankara basin, Turkey. J Appl Geophys 83:120–134. https://doi.org/10.1016/j.jappgeo.2012.05.007

Koçkar MK, Akgün H, Rathje EM (2010) Evaluation of site conditions for the Ankara Basin of Turkey based on seismic site characterization of near-surface geologic materials. Soil Dyn Earthq Eng 30:8–20. https://doi.org/10.1016/j.soildyn.2009.05.007

KOERI-RETMC (2020) Earthquake Catalog - BOUN KOERI Regional Earthquake-Tsunami Monitoring Center. http://www.koeri.boun.edu.tr/sismo/2/earthquake-catalog/

Kondo H, Awata Y, Emre Ö, Doğan A, Özalp S, Tokay F, Yildirim C, Yoshioka T, Okumura K (2005) Slip distribution, fault geometry, and fault segmentation of the 1944 Bolu-Gerede earthquake rupture, North Anatolian fault, Turkey. Bull Seismol Soc Am 95:34–49. https://doi.org/10.1785/012000440194

Lettis W, Bachhuber J, Witter R, Brankman C, Randolph CE, Barka A, Page WD, Kaya A (2002) Influence of releasing step-overs on surface fault rupture and fault segmentation: examples from the 17 August 1999 Izmit earthquake on the North Anatolian fault, Turkey. Bull Seismol Soc Am 92:19–42

Mori F, Mendicelli A, Moscatelli M, Romagnoli G, Peronace E, Naso G (2020) A new Vs30 map for Italy based on the seismic microzonation dataset. Eng Geol 275:1. https://doi.org/10.1016/j.enggeo.2020.105745

MTA (2003) Surface rupture associated with the August 17, 1999 İzmit earthquake, vol 1. Special Publications Series

MTA and Ankara University (1999) Geological Assessment of Alternative Settlement areas for Düzce Province Following 17 August 1999, TÜBİTAK, Earth-Sea-Atmosphere Sciences. and Environment Research Group Report, ANKARA

Nakamura Y (1989) A method for dynamic characteristics estimation of subsurface using microtremor on the ground surface. Q Rep Railw Tech Res Inst (RTRI) 30(1):273–281

Narayan JP, Kamal, (2018) A scenario of ground shaking hazard in intracratonic circular basins developed by basin-generated surface waves: an earthquake engineering perspective. Nat Hazards 92:1841–1857. https://doi.org/10.1007/s11069-018-3284-1

Núñez A, Rueda J, Mezcua J (2013) A site amplification factor map of the Iberian Peninsula and the Balearic Islands. Nat Hazards 65:461–476. https://doi.org/10.1007/s11069-012-0375-2

Okada H, Suto K (2003) The microtremor survey method. https://doi.org/10.1190/1.9781560801740

Özalaybey S, Zor E, Ergintav S, Tapirdamaz MC (2011) Investigation of 3-D basin structures in the İzmit Bay area (Turkey) by single-station microtremor and gravimetric methods. Geophys J Int 186:883–894. https://doi.org/10.1111/j.1365-246X.2011.05085.x

Özmen B (2000) Damage status of the 17 August 1999 Izmit Bay earthquake (With numerical data), TDV/DR 010-53, Turkish Earthquake Foundation, 132 p **(in Turkish)**

Palyvos N, Pantosti D, Zabci C, D'Addezio G (2007) Paleoseismological evidence of recent earthquakes on the 1967 Mudurnu Valley earthquake segment of the North Anatolian fault zone. Bull Seismol Soc Am 97:1646–1661. https://doi.org/10.1785/0120060049

Park S, Elrick S (1998) Predictions of shear-wave velocities in southern California using surface geology. Bull Seismol Soc Am 88:677–685

Park CB, Miller RD, Xia J (1999) Multichannel analysis of surface waves. Geophysics 64:800–808. https://doi.org/10.1190/1.1444590

Park CB, Miller RD, Rydén N, Xia J, Ivanov J (2005) Combined use of active and passive surface waves. J Environ Eng Geophys 10:323–334

Park CB, Miller RD, Xia J, Ivanov JM (2007) Multichannel analysis of surface waves (MASW). Lead Edge 26:60–64

Pegah E, Liu H (2016) Application of near-surface seismic refraction tomography and multichannel analysis of surface waves for geotechnical site characterizations: a case study. Eng Geol 208:100–113. https://doi.org/10.1016/j.enggeo.2016.04.021

Piatti C, Foti S, Socco LV, Boiero D (2013) Building 3D shear-wave velocity models using surface waves testing: the Tarcento basin case history. Bull Seismol Soc Am 103:1038–1047. https://doi.org/10.1785/0120120089

Polat O, Haessler H, Cisternas A, Philip H, Eyidogan H, Aktar M, Frogneux M, Comte D, Gürbüz C (2002) The İzmit (Kocaeli), Turkey earthquake of 17 August 1999: previous seismicity, aftershocks, and seismotectonics. Bull Seismol Soc Am 92:361–375. https://doi.org/10.1785/0120000816

Pratt TL, Brocher TM, Weaver CS, Creager KC, Snelson CM, Crosson RS, Miller KC, Tréhu AM (2003) Amplification of Seismic Waves by the Seattle Basin, Washington State. Bull Seismol Soc Am 93(2):533–545. https://doi.org/10.1785/0120010292

Pucci S, Pantosti D, Barchi MR, Palyvos N (2007) A complex seismogenic shear zone: the Düzce segment of North Anatolian Fault (Turkey). Earth Planet Sci Lett 262:185–203. https://doi.org/10.1016/j.epsl.2007.07.038

Rahman MZ, Kamal ASMM, Siddiqua S (2018) Near-surface shear wave velocity estimation and V_{S30} mapping for Dhaka City, Bangladesh. Nat Hazards 92:1687–1715. https://doi.org/10.1007/s11069-018-3266-3

Rix GJ, Hebeler GL, Orozco MC (2002) Near surface vs profiling in the New Madrid Seismic Zone using surface wave methods. Seismol Res Lett 73(3):380–392

Rodríguez-Marek A, Bray JD, Abrahamson NA (2001) An empirical geotechnical seismic site response procedure. Earthq Spectra 17(1):65–87. https://doi.org/10.1193/1.1586167

Roy N, SankarJakka R, Wason HR (2013) Effect of surface wave inversion non-uniqueness on 1D seismic ground response analysis. Nat Hazards 68:1141–1153. https://doi.org/10.1007/s11069-013-0677-z

Seligson CD (1970) Comments on high-resolution frequency-wavenumber spectrum analysis. Proc IEEE. https://doi.org/10.1109/PROC.1970.7825

SESAME (2004) Guidelines for the Implementation of the H/V Spectral Ratio Technique on Ambient Vibrations. Measurements, Processing and Interpretation, European Commission – Research General Directorate Project No. EVG1-CT- 2000–00026 SESAME, report D23.12. http://SESAME-FP5.obs.ujf-grenoble.fr

Şimşek O, Dalgıç S (1997) Düzce Ovası killerinin konsolidasyon özellikleri ve jeolojik evrim ile ilişkisi. Geol Bull Turkey 40:29–38 (**in Turkish**)

Singh AP, Mishra OP, Rastogi BK et al (2011) 3-D seismic structure of the Kachchh, Gujarat, and its implications for the earthquake hazard mitigation. Nat Hazards 57:83–105. https://doi.org/10.1007/s11069-010-9707-2

Takahashi T (2004) International society for the rock mechanics commision on application of geophysics to rock engineering suggesting methods for land geophysics in rock engineering. Int J Rock Mech Min Sci 41:885–914

Taymaz T (2000) Seismotectonics of the Marmara region: source characteristics of 1999 Gölcük-Sapanca-Düzce earthquakes. In: Proceedings of ITU-IAHS, international conference on the Kocaeli earthquake 17 August 1999, 2–5 December 1999. Istanbul, pp 55–78

Telford WM, Geldart LP, Sheriff RE, Keys DA (1976) Applied geophysics, 1st edn. Cambridge University Press, New York

Tokimatsu K (1995) Geotechnical Site characterization using surface waves. In: Proceedings, first international conference on earthquake geotechnical engineering, IS-Tokyo '95, Tokyo, Balkema, Rotterdam, pp 1333–1368

Uebayashi H, Kawabe H, Kamae K (2012) Reproduction of microseism H/V spectral features using a three-dimensional complex topographical model of the sediment-bedrock interface in the Osaka sedimentary basin. Geophys J Int 189:1060–1074. https://doi.org/10.1111/j.1365-246X.2012.05408.x

Utkucu M, Nalbant SS, McCloskey J, Steacy S, Alptekin Ö (2003) Slip distribution and stress changes associated with the 1999 November 12, Düzce (Turkey) earthquake (Mw = 7.1). Geophys J Int. https://doi.org/10.1046/j.1365-246X.2003.01904.x

Wang M, Hubbard J, Plesch A, Shaw JH, Wang L (2016) Three-dimensional seismic velocity structure in the Sichuan basin, China. J Geophys Res Solid Earth 121:1007–1022. https://doi.org/10.1002/2015JB012644

Wills CJ, Petersen M, Bryant WA, Reichle M, Saucedo GJ, Tan S, Taylor G, Treiman J (2000) A site-conditions map for California based on geology and shear-wave velocity. Bull Seismol Soc Am 90:187–208. https://doi.org/10.1785/0120000503

Wills CJ, Gutierrez CI, Perez FG, Branum DM (2015) A next generation Vs30 map for California based on geology and topography. Bull Seismol Soc Am 105:3083–3091. https://doi.org/10.1785/0120150105

Yoon S, Rix GJ (2004) Combined active-passive surface wave measurements for near surface site characterization. In: SAGEEP 2004, San Antonio, USA, pp 1556–1564

Yousefi-Bavil K (2022) Evaluation of site effects based on the 1999 Kocaeli and Düzce Earthquake events and seismic microzonation of Gölyaka, Düzce, Turkey, Ph.D. Dissertation, Middle East Technical University

Yousefi-Bavil K, Koçkar M K, Akgün H (2018) Development of a 3-D topographical basin structure based on seismic and geotechnical data: Case study at a high seismicity area of Gölyaka, Düzce, Turkey. In: Proceedings of the 16th European conference on earthquake engineering, Thessaloniki, Greece, Paper No. 11507